THE JOURNAL OF PHYSICAL CHEMISTRY C

Article

Cite This: J. Phys. Chem. C 2019, 123, 22564−22569

pubs.acs.org/JPCC

Unsupervised Exploration of MoS_2 Nanocluster Configurations: Structures, Energetics, and Electronic Properties

Mathieu Moog,*[,†] Sofiane Schaack,[‡] Fabio Pietrucci,[†] and A. Marco Saitta[†,¶]

[†]Sorbonne Université, UMR CNRS 7590, Muséum National d'Histoire Naturelle, Institut de Recherche pour le Développement, Institut de Minéralogie, de Physique des Matériaux et de Cosmochimie, 75252 Paris, France

[‡]Sorbonne Université, CNRS UMR 7588, Institut des NanoSciences de Paris (INSP), 75005 Paris, France

[¶]CNR, IPCF, Viale Ferdinando Stagno d'Alcontres 37, I-98158 Messina, Italy

Supporting Information

ABSTRACT: We propose an efficient method to explore the configuration space of nanoclusters by combining together ab initio molecular dynamics, metadynamics, and data clustering algorithms. On the one side, we employ collective variables sensitive to topological changes in the network of interatomic connections to map the configuration space; on the other side, we introduce an automatic approach to select, in such a space, representative structures to be optimized. In this way, we show that it is possible to sample thoroughly the set of relevant nanocluster geometries at a limited computational cost. We apply our method to explore MoS_2 clusters that recently raised a sizable interest due to their remarkable electronic and catalytic properties. We demonstrate that the unsupervised algorithm is able to find a large number of low-energy structures at different cluster sizes, including both bulk-like geometries and very different topologies. We are thus able to recapitulate, in a single computational study on technologically relevant MoS_2 clusters, the results of all previous works that employed distinct techniques like genetic algorithms or heuristic hypotheses. Furthermore, we found several new structures not previously reported. The ensemble of MoS_2 cluster structures is deposited in a publicly accessible database.

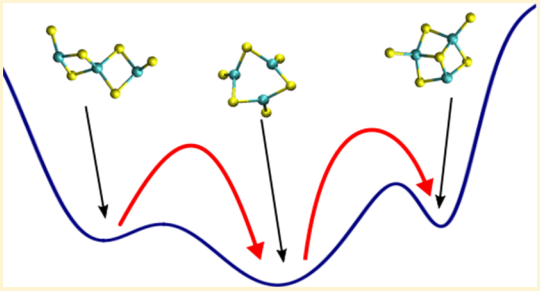

INTRODUCTION

In recent years, molybdenum−sulfur materials have been intensely studied by the scientific community for a range of applications[1] from hydrodesulfurization catalysts to transistors.[2−4] Interesting forms of this material go from the bulk to monolayers to nanostructures such as inorganic fullerenes[5] and nanoplatelets,[6−9] either recently synthesized or sought after.

For all these reasons, it is desirable to understand the formation mechanisms of Mo_nS_m nanostructures as well as their relationship with extended forms in terms of structure and properties. Consequently, this has been the focus of a number of experimental[8,10] and theoretical studies.[11−24] In some cases, W_nS_m and W_nO_m clusters have been studied in parallel with Mo_nS_m[11,13] due to the chemical similarity between the corresponding metals and chalcogens. Investigating different stoichiometries and cluster sizes provided indeed useful information: the so-called "magic clusters" seem to indicate a tendency to favor oversaturation in sulfur and monolayer-like structures with growing size rather than 3D arrangements.[6]

In most of the previous studies, the search for the possible structures of stable clusters was based on the enumeration of chemically intuitive geometries, using heuristic arguments or starting from the bulk material as a reference. This approach clearly is at high risk of missing important structures as hinted by the typically large energy gap between the most stable candidate found and the others. Moreover, it lacks objectivity and transferability to other systems. In fact, the importance of efficient and unbiased structural search algorithms in condensed matter in general and in nanostructures in particular is well appreciated.[25−27] In this respect, two recent studies used evolutionary algorithms to explore the configuration space of MoS_2[24] (although the search was supplemented in this case by arbitrary human-provided structures ex post) and WS_2 clusters.[23]

In this work, we propose an alternative sampling strategy, based on ab initio MD simulations, accelerated with metadynamics.[28] Finite temperature-enhanced sampling approaches have become widespread as they allow the exploration of generic transformation mechanisms in chemistry, physics, and biology, irrespective of the height of free-energy barriers.[29,30] However, their application to nanostructures is still sporadic, albeit successful.[31−35] A problem related to the exploration of the configuration space with enhanced sampling consists of finding suitable unsupervised procedures to select a limited number of representative geometries from finite T trajectories, which are further relaxed to identify local energy minima, thus providing candidates for stable clusters.

Received: May 20, 2019
Revised: August 9, 2019
Published: August 29, 2019

DOI: 10.1021/acs.jpcc.9b04763
J. Phys. Chem. C 2019, 123, 22564−22569

Here, we address this task exploiting a density clustering procedure initially introduced for protein structure classification,[36] obtaining in this way an automated protocol. Both for metadynamics and for classification, the atomic structure is described by topological collective variables ("social permutation invariant" (SPRINT) coordinates)[31] that are able to track the changes of interatomic bond networks in a range of condensed matter systems. These variables have been effectively employed in the literature both for exploration[32,37−40] and classification of structures.[41−43]

Overall, our methodology has several advantages. It requires a very limited number of parameters: essentially, the typical interatomic distances required to define SPRINT coordinates, the shape of the metadynamics repulsive Gaussians, and the granularity of the density clustering (see the Methods section for details). For this reason, we expect this protocol to be readily transferable to many other types of nanostructures. In addition, it also provides an identification of transition pathways, between different metastable structures, a "by-product" inherent to the use of MD trajectories, which can be of great interest for experimental synthesis. Finally, this method has a limited computational cost on current hardware. We showcase the efficiency of our method by applying it to three different cluster sizes: Mo_2S_4, Mo_3S_6, and Mo_4S_8.

METHODS

We started by running long exploratory ab initio Born−Oppenheimer MD simulations using the CPMD[44] code accelerated by metadynamics[28] as implemented in the PLUMED plugin.[45] We used DFT in the Perdew−Burke−Ernzerhof approximation,[46] employing Goedecker−Teter−Hutter pseudopotentials to describe core electrons,[47,48] a 1 fs timestep and a kinetic energy cutoff of 120 Ry with a convergence of 10^{-5} Ry.

The metadynamics trajectories were stored every 5 fs. For each cluster size, several independent trajectories were generated, starting from random initial atomic positions in a cubic periodically repeated box of 12 Å side with the objective that they lasted at least as long as 100 ps, to explore the space from different initial conditions. In all, we launched 4 simulations for Mo_2S_4, 8 simulations for Mo_3S_6, and 18 simulations for Mo_4S_8 (in this case, several simulations stopped under 20 ps being trapped in high energy states). By adding together all trajectories of the same cluster sizes, their total lengths reached 250 ps for Mo_2S_4, 900 ps for Mo_3S_6, and 1200 ps for Mo_4S_8 adding up to an overall length of 2.35 ns.

In metadynamics, the exploration of the configuration space is accelerated by means of a history dependent potential built as a sum of Gaussian repulsive functions deposited along the trajectory projected on collective variables (CVs). The efficiency of the algorithm is therefore highly dependent on the choice of CV that must be able to track all possible structural transformations of interest. In this work, we used the SPRINT collective variables,[31] based on graph theory, able to capture the "social" behavior of atoms in terms of the topology of the network of interatomic bonds. Starting from the interatomic distance matrix of the system, a sigmoid function decaying from 1 to 0 is applied to each distance d_{ij} between atoms i and j

$$\delta(d_{ij}) = \frac{1 - \left(\frac{d_{ij}}{d_0}\right)^m}{1 - \left(\frac{d_{ij}}{d_0}\right)^n} \quad (1)$$

with the parameters set to $d_0 = 4.5$ Å, $m = 8$, and $n = 24$ based on the pair correlation function of a cluster, computed using short (2 ps) and unbiased molecular dynamics simulations, to include up to the second nearest neighbor.

The resulting adjacency matrix is diagonalized, and SPRINT CVs are defined based on the largest eigenvalue and the corresponding eigenvector as

$$S_i = \sqrt{N}\lambda^{\max}\nu_i^{\max,\text{sorted}} \quad (2)$$

where N is the number or atoms.

The resulting positive values, one per atom, are sorted (keeping Mo and S separated) to enforce invariance by permutation of atoms of the same type. We applied N-dimensional Gaussian-shaped repulsive potentials of a height of 0.04 kJ·mol^{-1} and a width σ of 0.7, added every 10 fs. Those parameters were chosen after some short (less than 2 ps) molecular dynamics test simulations in which we did manage both to fill the initial potential wells, and we saw drops in bias potential, indicating exploration of new wells corresponding to potential stable structures.

The atomic trajectory projected in the N-dimensional SPRINT space is then classified using the algorithm proposed by Daura et al.[36] as implemented in the piv_clustering code.[49] The algorithm depends on a single parameter, a cutoff distance (d_c) in the SPRINT space defining whether two points are neighbor and thus determining the granularity of the clustering. We adopted $d_c = 0.3$ for Mo_2S_4, 0.6 for Mo_3S_6, and 1.2 for Mo_4S_8. Those parameters were chosen to generate a manageable number of candidate structures and were scaled with the dimension of the SPRINT collective variables. The classification resulted in 254 Mo_2S_4, 130 Mo_3S_6, and 178 Mo_4S_8 clusters.

The resulting candidate structures were then first partly optimized with a kinetic energy cutoff of 60 Ry for the wavefunction and 720 Ry for the density and a convergence criterion on the forces of 10^{-3} a.u. Next, duplicates and structures failing to relax were deleted. The remaining structures were further relaxed with a kinetic energy cutoff of 120 Ry for the wavefunction and 1440 Ry for the density, with a convergence criterion of 10^{-3} a.u. on the forces to obtain the final geometries, binding energies, HOMO−LUMO gaps, and magnetizations. The relaxations were run with Quantum Espresso[50] with the PBE[46] functional and Rappe−Rabe−Kaxiras−Joannopoulos ultrasoft pseudopotentials[51] in a cubic periodically repeated box of 15 Å side. Spin polarization effects were taken into account in the final relaxation to compute the magnetization.

Finally, to provide an estimate of the cost of the method, we computed the average computational cost of a 100 ps metadynamics simulation (Figure 1) as a function of the cluster size. Indeed, we expect that the cost of the metadynamics outweighs the cost of the relaxations and therefore is the determining factor. From Figure 1, it is clear that the cost of the method steeply increases with the size of the clusters and is in general too expensive for a local workstation but largely accessible for current supercomputers. Note that the cost of a single step varies significantly over a 100 ps simulation, notably because metadynamics forces the

DOI: 10.1021/acs.jpcc.9b04763
J. Phys. Chem. C 2019, 123, 22564−22569

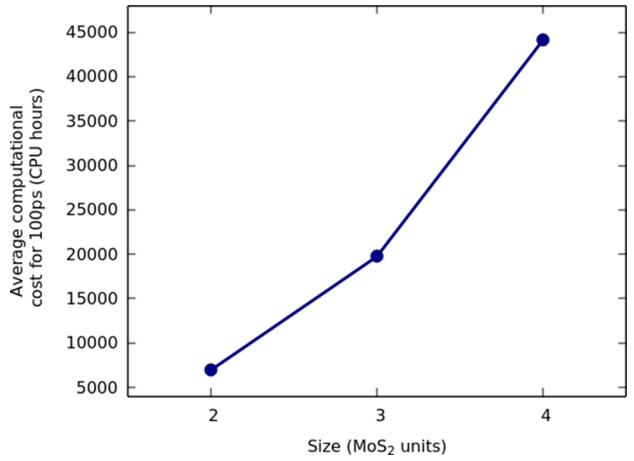

Figure 1. Average computational cost of 100 ps of simulation (in CPU hours) using Intel Xeon E5-2600 v3 Haswell processors as a function of the size of the cluster.

system to visit states of progressively higher energy; therefore, Figure 1 only gives a rough idea of the cost of those simulations.

RESULTS

Following the procedure outlined in the Methods section, we singled out more than 109 stable forms: 14 clusters for Mo_2S_4, 27 clusters for Mo_3S_6, and 68 clusters for Mo_4S_8. To sort the structures in terms of stability, we computed the binding energy using

$$\mathrm{BE} = \frac{nE(\mathrm{Mo}) + mE(\mathrm{S}) - E(\mathrm{Mo}_n\mathrm{S}_m)}{n+m} \quad (3)$$

where $E(\mathrm{Mo})$ and $E(\mathrm{S})$ are the energies of a molybdenum and sulfur atom, respectively, computed in the same conditions as the cluster, and $E(\mathrm{Mo}_n\mathrm{S}_m)$ is the energy of the $\mathrm{Mo}_n\mathrm{S}_m$ cluster. This definition has the advantage to allow energetic comparison of clusters with different numbers of atoms. For each n, we rank the structures in increasing BE, as n.BE_rank, for example, the fifth most stable structure of the Mo_3S_6 family will be referred to as 3.5.

The eight most stable structures and their binding energy relative to the most stable candidate are shown in Figures 2−4, with their binding energy, HOMO−LUMO gap, and total magnetization.

The observations of the most stable structures confirm what has been found elsewhere:[24] for n = 3 and n = 4, the most stable candidate has the form of the monolayer 1T phase of MoS_2. We observe a clear tendency for clusters to form platelet-like structures instead of core−shell ones. It is also noteworthy that we find several structures predicted using an evolutionary algorithm on WS_2.[23]

In addition we found several motifs (Figure 6) shared by many of the stable structures (indicated by colored squares in Figures 2−5): a Mo-centered tetrahedron with S atoms on the edges, a "core" of three or four Mo atoms bonded to each other and capped with sulfur atoms, and finally, an S-capped five-membered rings composed of two nonbonded S atoms and three Mo atoms.

A few structures, although less energetically favored (Figure 5), do stand out from the others, as they present original motifs such as a ring-like structure (2.13), the beginning of an

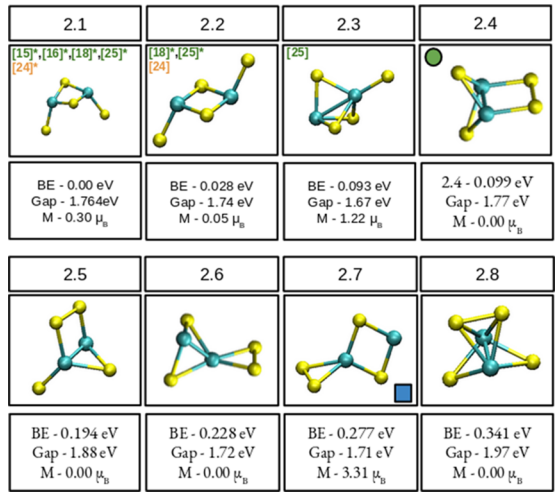

Figure 2. Most stable configurations for Mo_2S_4 clusters. Green and orange numbers refer to the references where the configurations were found, in MoS_2 (green) or WS_2 (orange) clusters, and asterisks indicate the structure identified as the most stable in the respective papers. Blue dots indicate a bulk-like structure. The blue square refers to the motif in Figure 6.

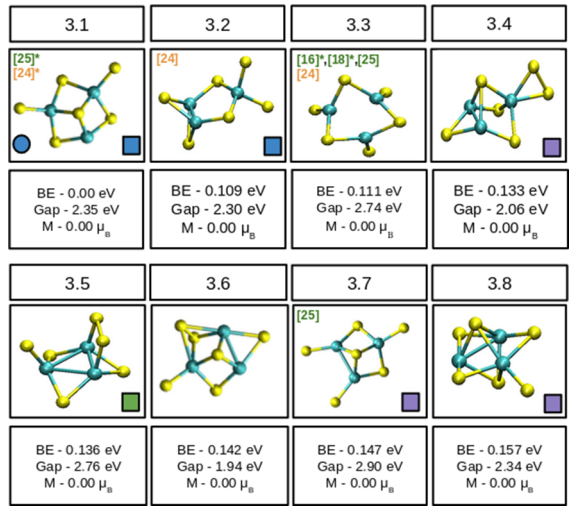

Figure 3. Most stable configurations for Mo_3S_6 clusters. Green and orange numbers and blue dots have the same meaning as the labels in Figure 2. Blue, violet, and green squares refer to the motifs in Figure 6.

MoS_2 1D structure (3.10), a structure with a S−S−S chain on an otherwise stable structure (4.20), and an interesting platelet-like structure that does not match the proposed structure of phase 1H or 1T (4.21). We also found some structures such as (2.10) or (3.10) that presented an interesting tetrahedron motif with two S atoms and two Mo atoms, bonded by their Mo−Mo edges, and in the case of 2.10, forming an octahedron with Mo atoms at opposite vertices.

DISCUSSION

From an energetic point of view, although the difference in methodology makes it difficult to make straightforward comparison with other works, we do find the same general trend with growing size[14,15,17] (Figure 7): larger structures are favored, and the binding energy of the clusters as a function of

DOI: 10.1021/acs.jpcc.9b04763
J. Phys. Chem. C 2019, 123, 22564−22569

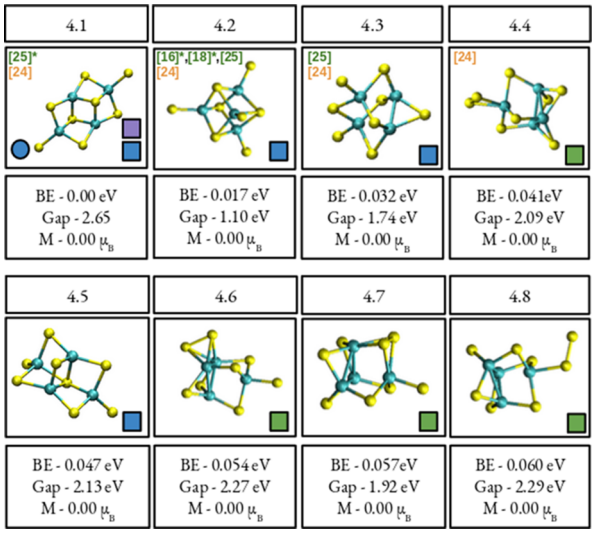

Figure 4. Most stable configurations for Mo_4S_8 clusters. Green and orange numbers and blue dots have the same meaning as the labels in Figure 2. Blue, violet, and green squares refer to the motifs in Figure 6.

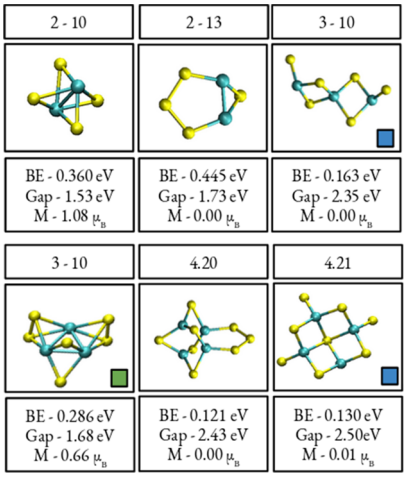

Figure 5. Interesting structures that are not among the eight most stable structures of each family *n*. Blue and green squares refer to the motifs in Figure 6.

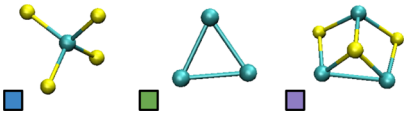

Figure 6. Geometric units appearing in several of the stable MoS_2 structures: the Mo-centered tetrahedron (left), the Mo core (center), and the S-capped five-membered ring (right).

their size seems to be increasing toward that of the bulk (Figure 7).

We find (Figure 7) that the structures of the smaller clusters are generally more spaced out than those of the larger clusters in binding energy. This also occurs when computing the number of structures within 2 eV (in absolute energy) of the most stable structure for each cluster size: we find 6 structures for Mo_2S_4, 15 structures for Mo_3S_6, and 35 structures for Mo_4S_8. However, we do note a very large absolute energy difference between the most stable and the second most stable

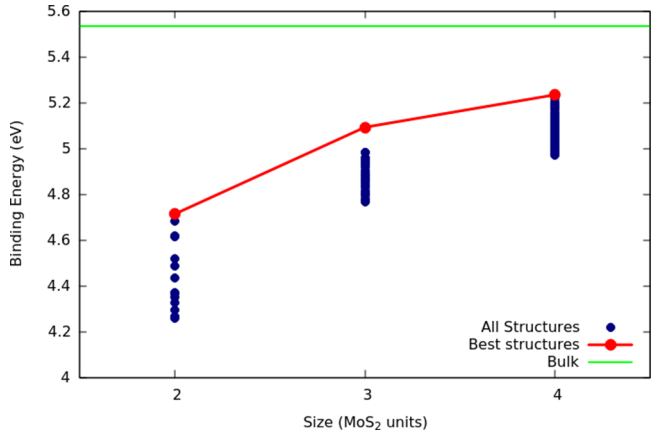

Figure 7. Evolution of the binding energy (eV) of the most stable configuration with increasing size (in MoS_2 units), with the binding energy of the bulk for comparison.

configurations of Mo_3S_6 clusters (0.97 eV), as opposed to 0.17 eV for Mo_2S_4 and 0.20 eV for Mo_4S_8.

We observe, in general, the same energy ranking as in previous works,[24] with one exception where structure 4.3 is found to be more stable than 4.2.[24] However, in this case, the differences in energy are small: 0.22 on the one hand[24] and 0.27 eV in our case and might be attributed to small structural differences and/or the use of different DFT functionals.

Despite differences in computational approaches, we find a general agreement with other studies on the magnetic nature of a cluster (magnetic vs nonmagnetic), although we find some important differences in the values of the reported magnetization. Comparing our results for the most common structures in the literature for the three sizes (structures 2.1, 3.3, and 4.2), we find an agreement with all other works for the two largest structures (3.3 and 4.2), which are reported as nonmagnetic,[15,17,24] however for the smallest cluster size the reported value is all cases $2\mu_B$,[15,17,24] while we find $0.3\mu_B$. It is quite likely that this discrepancy is due to the difference of methods used to take into account spin polarization.

For the HOMO−LUMO gap, we find a general agreement on the order of magnitude of the gap, although some discrepancies are also observed here: for cluster 2.1, the reported values of the HOMO−LUMO gap are 1.64,[14] 0.35,[15,17] 1.66 eV,[24] while our reported value is 1.74 eV; for structure 3.3, reported values are 0.7[18] and 2.11 eV[25] against our reported value of 2.7 eV. Finally, in Mo_4S_8, for structure 4.2, we find a HOMO−LUMO gap of 2.10 eV, while the literature contains values of 0.38[15,17] and 1.54 eV.

We note that the approximation level of electronic structure description employed in this study (DFT-PBE) is a good compromise between energetic accuracy and computational cost, given our approach based on long molecular dynamics trajectories. In this respect, our study is focused on the prejudice-free exploration of a large number of cluster structures (we provide the geometries in the Supporting Information as a reference for the scientific community), whereas a very accurate evaluation of energetics and electronic properties demands expensive, higher-level quantum chemistry approaches that go beyond the scope of this work.

CONCLUSIONS

In summary, we demonstrate that ab initio molecular dynamics in combination with enhanced sampling, data clustering, and

DOI: 10.1021/acs.jpcc.9b04763
J. Phys. Chem. C 2019, 123, 22564−22569

graph theory-inspired coordinates (SPRINT) capturing the topology of the interatomic network is a powerful approach for the unsupervised exploration of the configuration space of small clusters.

Indeed, in the case of Mo_nS_{2n} clusters, we recapitulated most the existing literature and discovered more than 50 new stable structures, making neither any guess about their geometry nor any assumption about their symmetry. We remark the excellent agreement of the structural forms found in this study with those observed in a previous study[23] using a very different exploration approach based on evolutionary algorithms.

In perspective, the unsupervised exploration of the configuration space of larger structures and/or different stoichiometries of Mo_nS_m clusters will constitute a very interesting field of research. Moreover, our proposed method could be seamlessly applied to other types of nanostructures and chemical compositions.

■ ASSOCIATED CONTENT

Supporting Information

The Supporting Information is available free of charge on the ACS Publications website at DOI: 10.1021/acs.jpcc.9b04763.

All structures related to this papers are provided in .xyz format (one per cluster size), along with the computed binding energies, absolute and total magnetization, and HOMO−LUMO gap, which are given in a .dat file (per cluster size) (ZIP)

■ AUTHOR INFORMATION

Corresponding Author

*E-mail: mathieu. moog@sorbonne-universite.fr.

ORCID

Mathieu Moog: 0000-0002-3003-7707

Notes

The authors declare no competing financial interest.

■ ACKNOWLEDGMENTS

This work was granted access to the HPC resources of TGCC, CINES, and IDRIS under the allocations 2018-A0040901387 and 2018-A0050910143 attributed by Grand Equipement National de Calcul Intensif (GENCI). This work was also granted access to the HPC resources of the HPCaVe Centre at Sorbonne Université.

■ REFERENCES

(1) Gemming, S.; Seifert, G.; Bertram, N.; Fischer, T.; Götz, M.; Ganteför, G. Onedimensional $(Mo_3S_3)_n$ clusters: Building blocks of clusters materials and ideal nanowires for molecular electronics. *Chem. Phys. Lett.* **2009**, *474*, 127−131.

(2) Yoon, Y.; Ganapathi, K.; Salahuddin, S. How good can monolayer MoS_2 transistors be? *Nano Lett.* **2011**, *11*, 3768−3773.

(3) Radisavljevic, B.; Radenovic, A.; Brivio, J.; Giacometti, V.; Kis, A. Single-layer MoS_2 transistors. *Nat. Nanotechnol.* **2011**, *6*, 147.

(4) Yin, Z.; Li, H.; Li, H.; Jiang, L.; Shi, Y.; Sun, Y.; Lu, G.; Zhang, Q.; Chen, X.; Zhang, H. Single-layer MoS_2 phototransistors. *ACS Nano* **2012**, *6*, 74−80.

(5) Pietsch, S.; Dollinger, A.; Strobel, C. H.; Park, E. J.; Ganteför, G.; Seo, H. O.; Kim, Y. D.; Idrobo, J.-C.; Pennycook, S. J. The quest for inorganic fullerenes. *J. Appl. Phys.* **2015**, *118*, 134302.

(6) Bertram, N.; Cordes, J.; Kim, Y. D.; Ganteför, G.; Gemming, S.; Seifert, G. Nanoplatelets made from MoS_2 and WS_2. *Chem. Phys. Lett.* **2006**, *418*, 36−39.

(7) Zhang, Z. J.; Zhang, J.; Xue, Q. J. Synthesis and characterization of a molybdenum disulfide nanocluster. *J. Phys. Chem.* **1994**, *98*, 12973−12977.

(8) Helveg, S.; Lauritsen, J. V.; Lægsgaard, E.; Stensgaard, I.; Nørskov, J. K.; Clausen, B. S.; Topsøe, H.; Besenbacher, F. Atomic-scale structure of single-layer MoS_2 nanoclusters. *Phys. Rev. Lett.* **2000**, *84*, 951.

(9) Li, T.; Galli, G. Electronic properties of MoS_2 nanoparticles. *J. Phys. Chem. C* **2007**, *111*, 16192−16196.

(10) Lauritsen, J. V.; Kibsgaard, J.; Helveg, S.; Topsøe, H.; Clausen, B. S.; Lægsgaard, E.; Besenbacher, F. Size-dependent structure of MoS_2 nanocrystals. *Nat. Nanotechnol.* **2007**, *2*, 53.

(11) Bertram, N.; Kim, Y. D.; Ganteför, G.; Sun, Q.; Jena, P.; Tamuliene, J.; Seifert, G. Experimental and theoretical studies on inorganic magic clusters: M_4X_6 (M = W, Mo, X = O, S). *Chem. Phys. Lett.* **2004**, *396*, 341−345.

(12) Seifert, G.; Tamuliene, J.; Gemming, S. Mo_nS_{2n+x} clusters—magic numbers and platelets. *Comput. Mater. Sci.* **2006**, *35*, 316−320.

(13) Gemming, S.; Seifert, G.; Götz, M.; Fischer, T.; Ganteför, G. Transition metal sulfide clusters below the cluster-platelet transition: theory and experiment. *Phys. Status Solidi B* **2010**, *247*, 1069−1076.

(14) Gemming, S.; Tamuliene, J.; Seifert, G.; Bertram, N.; Kim, Y. D.; Ganteför, G. Electronic and geometric structures of Mo_xS_y and W_xS_y (x = 1,2, 4; y =1-12) clusters. *Appl. Phys. A* **2006**, *82*, 161−166.

(15) Murugan, P.; Kumar, V.; Kawazoe, Y.; Ota, N. Ab initio study of structural stability of Mo-S clusters and size specific stoichiometries of magic clusters. *J. Phys. Chem. A* **2007**, *111*, 2778−2782.

(16) Murugan, P.; Kumar, V.; Kawazoe, Y.; Ota, N. Assembling nanowires from Mo-S clusters and effects of iodine doping on electronic structure. *Nano Lett.* **2007**, *7*, 2214−2219.

(17) Murugan, P.; Kumar, V.; Kawazoe, Y.; Ota, N. Atomic structures and magnetism in small MoS_2 and WS_2 clusters. *Phys. Rev. A* **2005**, *71*, No. 063203.

(18) Wang, B.; Wu, N.; Zhang, X.-B.; Huang, X.; Zhang, Y.-F.; Chen, W.-K.; Ding, K.-N. Probing the smallest molecular model of MoS_2 catalyst: S_2 Units in the $MoS_n^{-/0}$ (n = 1−5) Clusters. *J. Phys. Chem. A* **2013**, *117*, 5632−5641.

(19) Singh, D. M. D. J.; Pradeep, T.; Bhattacharjee, J.; Waghmare, U. V. Novel cage clusters of MoS_2 in the gas phase. *J. Phys. Chem. A* **2005**, *109*, 7339−7342.

(20) Mayhall, N. J.; Becher, E. L., III; Chowdhury, A.; Raghavachari, K. Molybdenum oxides versus molybdenum sulfides: geometric and electronic structures of $Mo_3X_y^-$(X = O, S and y = 6, 9) clusters. *J. Phys. Chem. A* **2011**, *115*, 2291−2296.

(21) Laraib, I.; Karthikeyan, J.; Murugan, P. First principles modeling of Mo_6S_9 nanowires via condensation of Mo_4S_6 clusters and the effect of iodine doping on structural and electronic properties. *Phys. Chem. Chem. Phys.* **2016**, *18*, 5471−5476.

(22) Patterson, M. J.; Lightstone, J. M.; White, M. G. Structure of Molybdenum and Tungsten Sulfide $M_xS_y^+$ Clusters: experiment and DFT Calculations. *J. Phys. Chem. A* **2008**, *112*, 12011−12021.

(23) Hafizi, R.; Hashemifar, S. J.; Alaei, M.; Jangrouei, M.; Akbarzadeh, H. Stable isomers and electronic, vibrational, and optical properties of WS_2 nano-clusters: A first-principles study. *J. Chem. Phys.* **2016**, *145*, 214303.

(24) Wang, Y.-Y.; Deng, J.-J.; Wang, X.; Che, J.-T.; Ding, X.-L. Small stoichiometric $(MoS_2)_n$ clusters with the 1T phase. *Phys. Chem. Chem. Phys.* **2018**, *20*, 6365−6373.

(25) Rossi, G.; Ferrando, R. Searching for low-energy structures of nanoparticles: a comparison of different methods and algorithms. *J. Phys.: Condens. Matter* **2009**, *21*, No. 084208.

(26) Pickard, C. J.; Needs, R. J. Ab initio random structure searching. *J. Phys.: Condens. Matter* **2011**, *23*, No. 053201.

(27) Oganov, A. R.; Lyakhov, A. O.; Valle, M. How Evolutionary Crystal Structure Prediction Works and Why. *Acc. Chem. Res.* **2011**, *44*, 227−237.

(28) Laio, A.; Parrinello, M. Escaping free-energy minima. *Proc. Natl. Acad. Sci. U. S. A.* **2002**, *99*, 12562−12566.

DOI: 10.1021/acs.jpcc.9b04763
J. Phys. Chem. C 2019, 123, 22564−22569

(29) Pietrucci, F. Strategies for the exploration of free energy landscapes: unity in diversity and challenges ahead. *Rev. Phys.* **2017**, *2*, 32−45.
(30) Camilloni, C.; Pietrucci, F. Advanced simulation techniques for the thermodynamic and kinetic characterization of biological systems. *Adv. Phys.: X* **2017**, *3*, 1477531.
(31) Pietrucci, F.; Andreoni, W. Graph theory meets ab initio molecular dynamics: atomic structures and transformations at the nanoscale. *Phys. Rev. Lett.* **2011**, *107*, No. 085504.
(32) Pietrucci, F.; Andreoni, W. Fate of a graphene flake: A new route toward fullerenes disclosed with ab initio simulations. *J. Chem. Theory Comput.* **2014**, *10*, 913−917.
(33) Pavan, L.; Di Paola, C.; Baletto, F. Sampling the energy landscape of Pt_{13} with metadynamics. *Eur. Phys. J. D* **2013**, *67*, 24.
(34) Pavan, L.; Rossi, K.; Baletto, F. Metallic nanoparticles meet metadynamics. *J. Chem. Phys.* **2015**, *143*, 184304.
(35) Tribello, G. A.; Giberti, F.; Sosso, G. C.; Salvalaglio, M.; Parrinello, M. Analyzing and driving cluster formation in atomistic simulations. *J. Chem. Theory Comput.* **2017**, *13*, 1317−1327.
(36) Daura, X.; Gademann, K.; Jaun, B.; Seebach, D.; Van Gunsteren, W. F.; Mark, A. E. Peptide folding: when simulation meets experiment. *Angew. Chem., Int. Ed.* **1999**, *38*, 236−240.
(37) Zheng, S.; Pfaendtner, J. Car-Parrinello molecular dynamics + metadynamics study of high-temperature methanol oxidation reactions using generic collective variables. *J. Phys. Chem. C* **2014**, *118*, 10764−10770.
(38) Wang, Y.; Huang, Y.; Gu, B.; Xiao, X.; Liang, D.; Rao, W. Formation of the $H_2SO_4 \cdot HSO^-_4$ dimer in the atmosphere as a function of conditions: a simulation study. *Mol. Phys.* **2016**, *114*, 3475−3482.
(39) Balan, E.; Pietrucci, F.; Gervais, C.; Blanchard, M.; Schott, J.; Gaillardet, J. Firstprinciples study of boron speciation in calcite and aragonite. *Geochim. Cosmochim. Acta* **2016**, *193*, 119−131.
(40) Fu, C. D.; Oliveira, L. F. L.; Pfaendtner, J. Assessing generic collective variables for determining reaction rates in metadynamics simulations. *J. Chem. Theory Comput.* **2017**, *13*, 968−973.
(41) Lai, J. Y. W.; Elvati, P.; Violi, A. Stochastic atomistic simulation of polycyclic aromatic hydrocarbon growth in combustion. *Phys. Chem. Chem. Phys.* **2014**, *16*, 7969−7979.
(42) Johansson, K. O.; Lai, J. Y. W.; Skeen, S. A.; Popolan-Vaida, D. M.; Wilson, K. R.; Hansen, N.; Violi, A.; Michelsen, H. A. Soot precursor formation and limitations of the stabilomer grid. *Proc. Combust. Inst.* **2015**, *35*, 1819−1826.
(43) Johansson, K. O.; Dillstrom, T.; Monti, M.; El Gabaly, F.; Campbell, M. F.; Schrader, P. E.; Popolan-Vaida, D. M.; Richards-Henderson, N. K.; Wilson, K. R.; Violi, A.; et al. Formation and emission of large furans and oxygenated hydrocarbons from flames. *Proc. Natl. Acad. Sci. U. S. A.* **2016**, *113*, 8374−8379.
(44) CPMD. *Copyright IBM Corp. 1990−2015, Copyright MPI für Festkörperforschung Stuttgart 1997−2001*. http://cpmd.org/.
(45) Bonomi, M.; Branduardi, D.; Bussi, G.; Camilloni, C.; Provasi, D.; Raiteri, P.; Donadio, D.; Marinelli, F.; Pietrucci, F.; Broglia, R. A.; et al. PLUMED: a portable plugin for free-energy calculations with molecular dynamics. *Comput. Phys. Commun.* **2009**, *180*, 1961−1972.
(46) Perdew, J. P.; Burke, K.; Ernzerhof, M. Generalized gradient approximation made simple. *Phys. Rev. Lett.* **1996**, *77*, 3865.
(47) Goedecker, S.; Teter, M.; Hutter, J. Separable dual-space Gaussian pseudopotentials. *Phys. Rev. B* **1996**, *54*, 1703.
(48) Krack, M. Pseudopotentials for H to Kr optimized for gradient-corrected exchange-correlation functionals. *Theor. Chem. Acc.* **2005**, *114*, 145−152.
(49) Gallet, G. A.; Pietrucci, F. Structural cluster analysis of chemical reactions in solution. *J. Chem. Phys.* **2013**, *139*, No. 074101.
(50) Giannozzi, P.; Baroni, S.; Bonini, N.; Calandra, M.; Car, R.; Cavazzoni, C.; Ceresoli, D.; Chiarotti, G. L.; Cococcioni, M.; Dabo, I.; Dal Corso, A.; et al. *J. Phys.: Condens. Matter* **2009**, *21*, 395502.
(51) Rappe, A. M.; Rabe, K. M.; Kaxiras, E.; Joannopoulos, J. D. Optimized pseudopotentials. *Phys. Rev. B* **1990**, *41*, 1227.

DOI: 10.1021/acs.jpcc.9b04763
J. Phys. Chem. C 2019, 123, 22564−22569